THE FASEB JOURNAL • RESEARCH • www.fasebj.org

Complement-induced activation of the cardiac NLRP3 inflammasome in sepsis

Miriam Kalbitz,*,† Fatemeh Fattahi,* Jamison J. Grailer,* Lawrence Jajou,* Elizabeth A. Malan,* Firas S. Zetoune,* Markus Huber-Lang,† Mark W. Russell,‡ and Peter A. Ward*,[1]

*Department of Pathology and ‡Department of Pediatric Cardiology, University of Michigan Medical School, Ann Arbor, Michigan, USA; and †Department of Orthopaedic Trauma, Hand, Plastic, and Reconstructive Surgery, University Hospital of Ulm, Ulm, Germany

ABSTRACT: Cardiac dysfunction develops during sepsis in humans and rodents. In the model of polymicrobial sepsis induced by cecal ligation and puncture (CLP), we investigated the role of the NLRP3 inflammasome in the heart. Mouse heart homogenates from sham-procedure mice contained high mRNA levels of NLRP3 and IL-1β. Using the inflammasome protocol, exposure of cardiomyocytes (CMs) to LPS followed by ATP or nigericin caused release of mature IL-1β. Immunostaining of left ventricular frozen sections before and 8 h after CLP revealed the presence of NLRP3 and IL-1β proteins in CMs. CLP caused substantial increases in mRNAs for IL-1β and NLRP3 in CMs which are reduced in the absence of either C5aR1 or C5aR2. After CLP, NLRP3$^{-/-}$ mice showed reduced plasma levels of IL-1β and IL-6. *In vitro* exposure of wild-type CMs to recombinant C5a (rC5a) caused elevations in both cytosolic and nuclear/mitochondrial reactive oxygen species (ROS), which were C5a-receptor dependent. Use of a selective NOX2 inhibitor prevented increased cytosolic and nuclear/mitochondrial ROS levels and release of IL-1β. Finally, NLRP3$^{-/-}$ mice had reduced defects in echo/Doppler parameters in heart after CLP. These studies establish that the NLRP3 inflammasome contributes to the cardiomyopathy of polymicrobial sepsis.—Kalbitz, M., Fattahi, F., Grailer, J. J., Jajou, L., Malan, E. A., Zetoune, F. S., Huber-Lang, M., Russell, M. W., Ward, P. A. Complement-induced activation of the cardiac NLRP3 inflammasome in sepsis. FASEB J. 30, 3997–4006 (2016). www.fasebj.org

KEY WORDS: C5a · C5a receptors · IL-1β · CLP

Over the past decade, the nucleotide-binding oligomerization domain–like receptor with pyrin domain (NLRP)-3 inflammasome has received a great deal of attention as an important mediator pathway of the innate immune system. It contains 3 components [NLRP3, caspase-1 and apoptosis-associated speck-like protein containing a caspase recruitment domain (ASC)]. Inflammasome activation by LPS (primer) followed by ATP (activator) results in caspase-1 activation, which causes cleavage of precursor forms of IL-1β and -18 into mature (cleaved) active cytokines that are then secreted. The chief products of the NLRP3 inflammasome, IL-1β, and -18, are strongly proinflammatory (1, 2). Other priming agents include intrinsic factors [danger-associated molecular patterns (DAMPs)], such as uric acid crystals, hyaluronan, amyloid fibrils, cholesterol crystals, and histones, which are released from damaged or inflamed tissues and from neutrophil extracellular traps (NETs) activated by C5a (3), resulting in NLRP3 inflammasome activation, damaging inflammatory responses that amplify tissue and organ damage (4–6). Furthermore, pathogen-associated molecular patterns (PAMPs) activate TLRs and the NLRP3 inflammasome (7, 8). Alternative activating agents include bacterial toxins (nigericin and maitotoxin) (9). Collectively, the NLRP3 inflammasome can provide protective responses in infectious and noninfectious situations, but excessive inflammasome activation often intensifies inflammatory injury.

During remodeling after myocardial ischemia and reperfusion, activation of the NLRP3 inflammasome in cardiac fibroblasts has been observed (10, 11), which was largely prevented in the absence of ASC or caspase-1 (11). As a consequence of events in the ischemic heart, release of proinflammatory mediators has been postulated to amplify myocardial injury (12, 13). Blockade of caspase-1 (12, 14), overexpression of IL-1R antagonist (15), or blockade of IL-1β with neutralizing antibody (16) have resulted in

ABBREVIATIONS: ASC, apoptosis associated speck-like protein containing a caspase recruitment domain; CLP, cecal ligation and puncture; C5a, complement component 5a; C5aR1, complement component 5a receptor 1; CM, cardiomyocyte; CO, cardiac output; DAMP, danger-associated molecular pattern; echo, echocardiography; E′sa, peak velocity from the septal annulus of the mitral valve; HR, heart rate; IL-1R, IL-1 receptor; KO, knockout; LV, left ventricle; NET, neutrophil extracellular trap; NOX, NADPH oxidase; NLRP3, nucleotide-binding oligomerization domain-like receptor with pyrin domain 3; PAMP, pathogen-associated molecular pattern; qPCR, quantitative real time PCR; rC5a, recombinant complement component 5a; ROS, reactive oxygen species; SV, stroke volume; VolS, volume at end systole; VolD, volume at end diastole

[1] Correspondence: University of Michigan Medical School, Department of Pathology, 1301 Catherine Rd., 7520 MSRB I, Box 5602, Ann Arbor, MI 48109-5602, USA. E-mail: pward@umich.edu

doi: 10.1096/fj.201600728R

protective effects in myocardial ischemia. In essence, in the ischemic heart tissue, proinflammatory products from NLRP3 inflammasome activation intensified cardiac injury.

After experimental burn trauma and during experimental cecal ligation and puncture (CLP), cardiomyocytes (CMs) have been shown to generate and release proinflammatory cytokines, such as TNF, IL-1β, and IL-6 (17, 18). CMs exposed *in vitro* to the complement anaphylatoxin C5a likewise release IL-1β and TNF (18). NLRP3 inflammasome activation was found to be essential in complement-mediated IL-1β release in murine dendritic cells (19) and human retinal pigment epithelial cells (20). Cytokines and C5a have both been shown to have cardiosuppressive effects (17, 21–23). Further, *in vitro* addition of C5a to rat CMs isolated from both sham-procedure and CLP animals causes dramatic cardiac dysfunction involving both contractility and relaxation (23) associated with overexpression of C5a receptor (C5aR) in CMs isolated after CLP (23). Furthermore, in experimental CLP sepsis, complement C5a receptor 1–knockout (KO) ($C5aR1^{-/-}$) and C5a receptor 2–KO ($C5aR2^{-/-}$) mice had survival rates superior to those of wild-type (WT) mice (24). C5a blockade or absence of either C5a receptor (C5aR1 or C5aR2) diminished development of cardiac dysfunction after thermal injury (25) or during experimental sepsis (26), respectively.

However, whether NLRP3 inflammasome activation in CMs during sepsis plays a role in development of cardiac dysfunction after sepsis and its precise relation to the C5a receptors are not clear. The current experiments provide novel evidence for the constitutive presence and activation of the NLRP3 inflammasome in CMs during polymicrobial sepsis in mice. The events are associated with release of IL-1β, which may contribute to the cardiac dysfunction of sepsis.

MATERIALS AND METHODS

Isolation of CMs

CMs were isolated from young adult rats and mice, according to published procedures (3, 18, 27, 28). In brief, after excision of the heart, the aorta ascendens was cannulated, and the hearts were fixed to a Langendorff perfusion system. The hearts were retrograde perfused with Liberase solution (Hoffmann-La Roche, Mannheim, Germany), according to the manufacturer's directions. After digestion, the heart was detached from the Langendorff apparatus; atria and vessels were removed, and the ventricles were cut into small pieces, which were gently triturated with a plastic transfer pipette. After isolation of the CMs, the Ca^{2+} concentration in the buffer fluid was gradually increased in 6 steps (to 1.8 mM) and the cells were cultured in M199 medium with 1% insulin-transferrin-selenium-X (Thermo Fisher Scientific, Waltham, MA, USA) including antibiotic-antimycotic (Thermo Fisher Scientific).

Animals and anesthesia

All procedures conformed to the *Guide for the Care and Use of Laboratory Animals* (National Institutes of Health, Bethesda, MD, USA). The study was approved by the University Committee on Use and Care of Animals and performed according to the guidelines. Specific pathogen-free male Sprague-Dawley rats (300–350 g; Harlan Laboratories, Indianapolis, IN, USA) and male C57BL/6 mice (6–10 wk, 25–30 g; The Jackson Laboratory, Bar Harbor, ME, USA) were anesthetized with the combination of ketamine (40 mg/kg body weight; Hospira, Lake Forest, IL, USA) and xylazine (5 mg/kg body weight; Lloyd Laboratories, Shenandoah, IA, USA) intraperitoneally. Some experiments were also performed using male C57BL/6 mice from our $C5aR1^{-/-}$ and $C5aR2^{-/-}$ breeding colonies at the University of Michigan. The generation of $C5aR1^{-/-}$ and $C5aR2^{-/-}$ mice on a C57BL/6 background has been described previously (29, 30). Male $NLRP3^{-/-}$ mice were purchased from The Jackson Laboratory.

Experimental sepsis

Sepsis was induced by the CLP procedure, as described previously (31). In anesthetized animals, a midline surgical incision was made, and the cecum was exposed and ligated at half the distance between the distal pole and the base of the cecum, resulting in a midgrade sepsis (32). The cecum was punctured, and a small amount of feces was expressed. The abdomen was closed in layers with 5-0 sutures (Ethicon, Inc., Somerville, NJ, USA). Sham-procedure animals underwent the same procedure, including manipulation of the bowel in the absence of CLP. In all animals, 3.0 ml (rats) or 1.0 ml (mice) fluid resuscitation (lactated Ringers solution) was injected given subcutaneously in the nuchal region, after surgery. Fluids were given immediately (0 h) and 12 h after CLP. The animals were euthanized 8, 12, 16, 18, 24, or 48 h after CLP.

Measurement of ROS

Intracellular ROS in rat CMs was measured by flow cytometry using CellRox dyes (Thermo Fisher Scientific) according to the manufacturer's directions. The dyes detect either cytoplasmic or mitochondrial ROS. A minimum of 10,000 events was observed on a BD LSR II flow cytometer (BD Biosciences) and analyzed with FlowJo Software 7.6.4 (Tree Star, Ashland, OR, USA). Dot plots and figures show ≥10,000 events.

Confocal imaging

For confocal imaging, CMs were cultured on sterile glass slides coated with natural mouse laminin (Thermo Fisher Scientific) stained with CellRox Deep Red or Deep Green Reagent. These dyes are cell and mitochondrion permeable. NLRP3 and IL-1β staining was performed on mouse frozen left ventricle (LV) tissue sections. For NLRP3 staining monoclonal rat anti-mouse was used as primary (R&D Systems, Inc., Minneapolis, MN, USA) and donkey anti-rat (AF-647) as secondary antibody (Jackson ImmunoResearch Laboratories, West Grove, PA, USA). For IL-1β staining, rabbit anti-mouse antibody was used as primary (Abcam, Inc., Cambridge, MA, USA) and donkey anti-rabbit (AF-488) as secondary antibody (Jackson ImmunoResearch Laboratories). After staining, cells/sections were washed twice with PBS and covered with ProLong Gold Antifade Reagent (Thermo Fisher Scientific). Confocal imaging was performed by the LSM 510 Confocal microscope (Zeiss, Thornwood, NY, USA) in the Microscopy and Image-Analysis Laboratory (Department of Cell and Developmental Biology, University of Michigan Medical School).

IL-6 and IL-1β ELISA

Supernatants of cultured rat CMs were collected and analyzed using ELISA kits (R&D Systems) to measure IL-1β. In some experiments, blood from WT and $NLRP3^{-/-}$ mice was collected

through cardiac puncture using anticoagulant citrate dextrose solution at different time points after CLP, and the plasma was analyzed using ELISA kits (R&D Systems) to measure IL-6 and mature IL-1β according to the manufacturer's instructions.

NLRP3, caspase-1 and IL-1β in mouse heart homogenates and CMs by RT-PCR

Mouse hearts (isolation as described above) were obtained after CLP or the sham procedure and harvested at various times. Total RNA was isolated by the Trizol method (Thermo Fisher Scientific) according to the manufacturer's instructions. RNA was obtained and amplified (SYBR) using reagents from Thermo Fisher Scientific. RT-PCR amplification was performed on a 7500 Real-Time PCR System (Thermo Fisher Scientific). Calculation of the relative quantitative results was performed according to the $2^{-\Delta\Delta Ct}$ algorithm.

The following mouse primers were used: NLRP3 5′GCTGCTCAGCTCTGACCTCT3′ (fwd), mouse NLRP3 5′-AGGTGAGGCTGCAGTTGTCT-3′ (rev); IL-1β 5′-TGAAAGCTCTCCACCTCAATGGAC-3′ (fwd), IL-1β 5′-TGCAGCCATCTTTAGGAAGACACG-3′ (rev); caspase-1 5′-CCAGAGCACAAGACTTCTGAC-3′ (fwd), caspase-1 5′-TGGTGTTGAAGAGCAGAAAGC-3′ (rev); mouse ASC-1 5′-GCAATGTGCTGACTGAAGGA-3′ (fwd), mouse ASC-1 5′-TGTTCCAGGTCTGTCACCAA-3′ (rev). For the housekeeping gene, 5′-CTTCAACAGCAACTCCCACTCTTCC-3′ (fwd), Gapdh 5′-GGTGGTCCAGGGTTTCTTACTCC-3′ (rev) was used.

Reagents

The following reagents were used: recombinant rat or mouse C5a (rC5a) with virtually no detectable LPS were produced as has been described (23, 33). Chemicals used for preparation of solutions for CM isolation; VAS-2870, used as an NADPH oxidase (NOX)-2 inhibitor; and Y-VAD as a global caspase-1 inhibitor were purchased from Sigma-Aldrich (St. Louis, MO, USA). Inhibitors were used in concentrations of 10 μM according to the literature.

Echocardiography

Echocardiography (echo) was performed as published (34). All echocardiograms were recorded by a registered echocardiographer who was blinded to mouse genotype. NLRP3$^{-/-}$ mice, together with WT C57Bl/6J mice, were weighed and anesthetized with inhaled isoflurane. Imaging was performed with a Vevo 770 High-Resolution In Vivo Imaging System (VisualSonics, Inc., Toronto, ON, Canada) equipped with an RMV-707, 30 MHz (Real-Time Visualization; up to 45 MHz) scanhead. LV volume at end systole (VolS) and volume at end diastole (VolD) were measured from the parasternal long-axis view at the level of the tips of the leaflets of the mitral valve at end systole and end diastole, respectively, and used to calculate stroke volume (SV) and ejection fraction (EF): SV = VolD − VolS and EF % = endocardial SV/endocardial VolD × 100. Cardiac output (CO) was calculated from SV and heart rate (HR): CO = SV × HR. Mitral valve E and A wave inflow velocities were sampled at the tips of the leaflets of the mitral valve from the apical 4-chamber view. Doppler tissue imaging was performed with acquisition of peak velocity (E′) from the lateral annulus (E′la) and septal annulus (E′sa) of the mitral valve, imaged from the apical 4-chamber view. Isovolumic relaxation time, from the closure of the aortic valve to the opening of the mitral valve, was measured from the apical 5-chamber view using Doppler flow imaging. Imaging was performed at 8 h after CLP.

Statistical analysis

For statistical analysis, Prism 6 (GraphPad, La Jolla, CA, USA) was used. All values are expressed as means ± SEM. Data were analyzed by 1-way ANOVA followed by Dunnett's multiple-comparison test. For comparison of 2 groups, the Student's t test was used. Values of $P \leq 0.05$ were considered significant.

RESULTS

Levels of inflammasome components and IL-1β in LV homogenates and responses of CMs to inflammasome protocols

qRT-PCR technology was used with mouse LV homogenates (**Fig. 1*A***) to measure inflammasome content (mRNAs for the 3 inflammasome components: NLRP3, caspase-1, and ASC) and IL-1β in resting cells. Results were expressed as a ratio to Gapdh mRNA, which was set at a value of 1.0. In LV homogenates from normal WT mouse hearts, the declining order of subunit content (mRNAs) was NLRP3 > caspase-1 = IL-1β > ASC. We used an

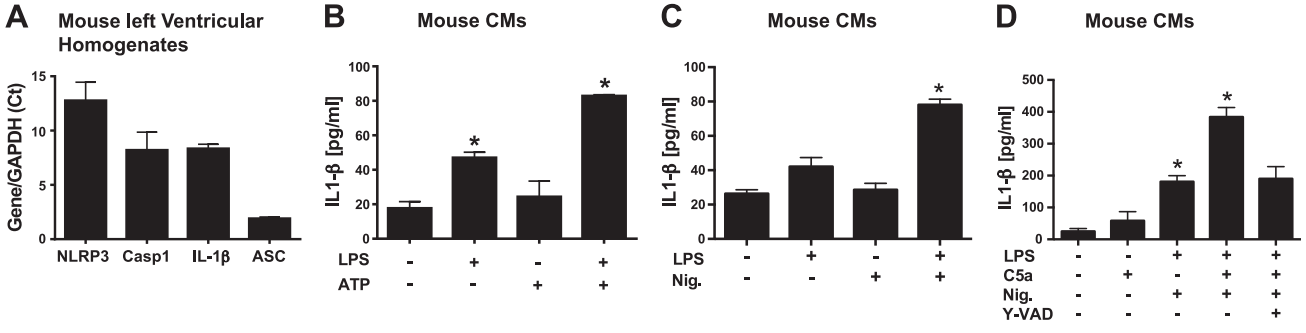

Figure 1. mRNA levels of inflammasome components in mouse heart homogenates and activation of NLRP3 inflammasome in CMs. *A*) Using LV homogenates from mouse hearts, mRNAs were measured for NLRP3, caspase-1, ASC, and IL-1β by qRT-PCR and developed as a ratio to mRNA for Gapdh (set as 1.0). *B*) Mouse CMs were incubated with buffer or with LPS (1 μg/ml for 4 h at 37°C) or the combination, with the endpoint being IL-1β release. *C*, *D*) CM release of IL-1β was measured after cell exposure to buffer or LPS (primer), followed by addition of activator (ATP or nigericin, 1 mM or 10 μm, respectively, for 45 min at 37°C). Where indicated, 10 μm Y-VAD, a global caspase inhibitor, was also used. For each bar, $n \geq 5$ samples. *$P < 0.05$

inflammasome protocol with the endpoint being release of mature IL-1β from rat CMs. CMs were exposed to buffer or to LPS for 4 h at 37°C (Fig. 1*B*), or they were exposed to the inflammasome activators ATP (1 mM) (Fig. 1*B*) or nigericin (10 μM) (Fig. 1*C*) for 45 min at 37°C. The ATP or nigericin caused release of IL-1β, same as baseline levels. Baseline levels of IL-1β were ~20 pg/ml. The presence of LPS alone was associated with doubling of IL-1β release from CMs compared to baseline release (Fig. 1*B*). When CMs were exposed to ATP or nigericin after incubation with LPS, IL-1β release from CMs rose to 80 pg/ml, indicating activation of NLRP3 inflammasome in CMs (Fig. 1*B*, *C*). In Fig. 1*D*, baseline levels of IL-1β release was small (~30 pg/ml), whereas the presence of C5a alone resulted in doubling the amount of IL-1β released (~50 pg/ml). The presence of LPS followed by nigericin caused greatly enhanced release of IL-1β, to ~180 pg/ml, whereas the initial presence of C5a with LPS followed by nigericin caused a synergistic release of IL-1β (380 pg/ml), suggesting a synergy in inflammasome activation when the initial priming agents were LPS+C5a, followed by nigericin as the activator agent. When the same conditions were used in the continuing presence of the pancaspase inhibitor, Y-VAD (10 μM), the release of IL-1β fell by 52%.

Activation of the NLRP3 inflammasome in LV CMs from CLP mice

We used immunofluorescence confocal microscopy to search for the NLRP3 inflammasome in frozen sections from the LVs of mouse hearts before (**Fig. 2**, ctrl sham) or 8 h after CLP (Fig. 2; magnification, ×63). Selection of the 8-h time point after CLP was based on our knowledge that, at this time, echo/Doppler parameters indicated the onset of cardiac dysfunction after sepsis (3). LV frozen sections from sham-procedure hearts revealed very faint amounts of IL-1β or NLRP3 protein, as detected by immunofluorescence (Fig. 2, ctrl sham). However, there was a greatly increased presence of IL-1β and NLRP3 protein in LV CMs from WT CLP hearts, as indicated by the green (IL-1β) or red (NLRP3) fluorescence, respectively. The presence of red fluorescence, denoting NLRP3 protein, occurred in a pattern similar to that for IL-1β. DAPI yielded blue-stained nuclei in CMs. The merge image produced a yellow fluorescence (coalescence of green and red colors), together with the blue nuclei that were clearly within the CMs, all of which were prominent in frozen longitudinal LV sections. Lower power images were obtained to determine whether NLRP3 protein was detectable in interstitial areas of the heart. Such evidence could not be found.

In sepsis, NLRP3 inflammasome activation in mouse CMs is reduced in absence of either C5aR1 or C5aR2

Mouse LV CMs were isolated before (control) or 8 to 16 h after polymicrobial sepsis from WT, C5aR1$^{-/-}$, and C5aR2$^{-/-}$ mice (**Fig. 3**). CMs were then evaluated for changes in mRNAs for components of the NLRP3 inflammasome and IL-1β. mRNAs for NLRP3, caspase-1, ASC, IL-1β, and Gapdh were quantitated by qRT-PCR and expressed as ratios to Gapdh in the same specimens. The fold change in sham-procedure heart was compared to Gapdh, which was set at 1.0 (not shown). There was an ~35-fold increase in mRNA for NLRP3 in CMs 8–16 h after sepsis (Fig. 3*A*). These increases were almost totally ablated in CMs from septic C5aR1$^{-/-}$ or C5aR2$^{-/-}$ mice. There were very small elevations (<1.5-fold) in LV mRNAs for caspase-1 after CLP (Fig. 3*B*). The slightly diminished increments for caspase-1 mRNAs in LV CMs from mice lacking either C5a receptor were not statistically different. The pattern for changes in ASC mRNA was very small and not statistically significant (Fig. 3*C*). LV mRNA for IL-1β rose nearly 80-fold 8 h after CLP in WT mice (Fig. 3*D*). Virtually no increase in mRNA for IL-1β was found in mice lacking either C5a receptors.

Absence of NLRP3 in CLP mice affects both IL-1β and IL-6 proteins

After CLP, we assessed plasma levels of IL-1β (as a marker of inflammasome activation) and IL-6, which is another heart-suppressive cytokine (**Fig. 4**). We determined the

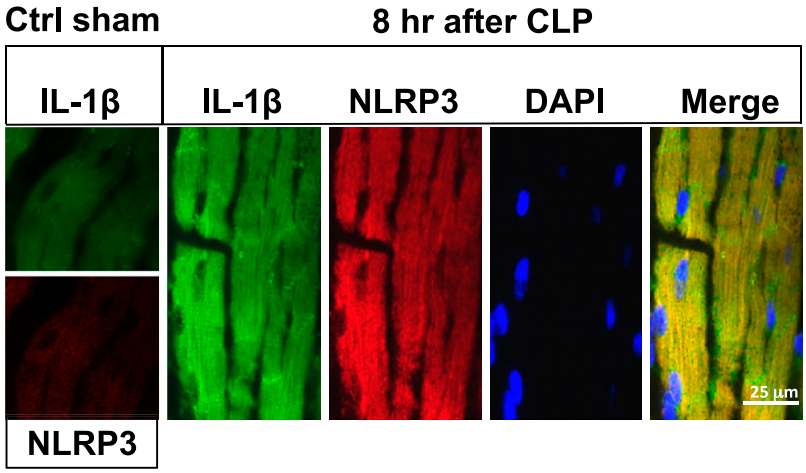

Figure 2. Activation of NLRP3 inflammasome in LV mouse CMs after CLP. Immunofluorescence analysis of LV frozen sections from sham-procedure cointrol (ctrl sham) mouse WT heart (left boxes) or hearts 8 h after CLP. Magnification, ×63. Analysis involved immunostaining for IL-1β (green), NLRP3 (red), nuclear staining by DAPI, and the merge image for all 3 stains. Staining for IL-1β and NLRP3 was very faint in sham-procedure control hearts, in striking contrast to hearts 8 h after CLP.

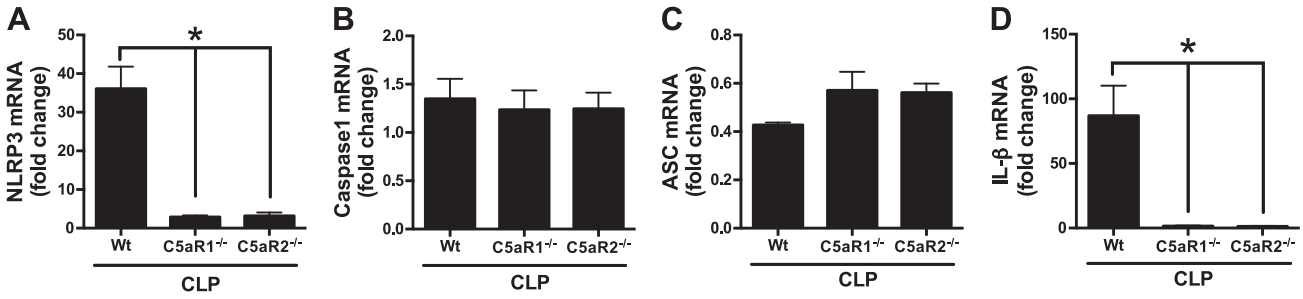

Figure 3. In sepsis, NLRP3 inflammasome activation in mouse CMs is reduced in absence of either C5aR1 or C5aR2. Activation of the NLRP3 inflammasome components NLRP3 (*A*), caspase-1 (*B*), and ASC (*C*), as well as IL-β (*D*), in mouse CMs before (not shown) and 16 h after CLP. In these studies, qRT-PCR was used in LV heart homogenates from WT, and C5aR1$^{-/-}$ or C5aR2$^{-/-}$, 16 h after CLP. Results are ratios of NLRP3 inflammasome component mRNA to Gapdh mRNA (the latter being set at 1.0). For each bar, $n \geq 4$ samples. *$P < 0.05$.

appearance of IL-1β in plasma from WT mice and found a sustained increase in IL-1β over the period of 8–24 h after CLP, although there was a pattern of gradual reduction of plasma IL-1β 18–24 h after CLP (Fig. 4*A*). We selected the 18-h interval after CLP in WT and NLRP3$^{-/-}$ mice for additional experiments. There was a 75% reduction for plasma IL-1β when compared to the levels of IL-1β in WT CLP mice (Fig. 4*B*). When plasma IL-6 was also measured in WT CLP mice, there was a gradual decline in plasma IL-6 at 12, 18, and 24 h after CLP (Fig. 4*C*). For plasma IL-6, the 8-h interval after CLP was selected, using WT and NLRP3-KO mice. The NLRP3-KO mice showed a 58% reduction in plasma IL-6 (Fig. 4*D*). It was clear that the absence of NLRP3 resulted in reduced plasma levels of both IL-1β and -6 after CLP.

Complement-dependent *in vitro* and *in vivo* induction of ROS in CMs

Fluorescent dyes were used that have been verified to distinguish between ROS in a nuclear/mitochondrial location and a cytosolic location (**Fig. 5**). In this series of experiments, confocal fluorescence microscopy was used

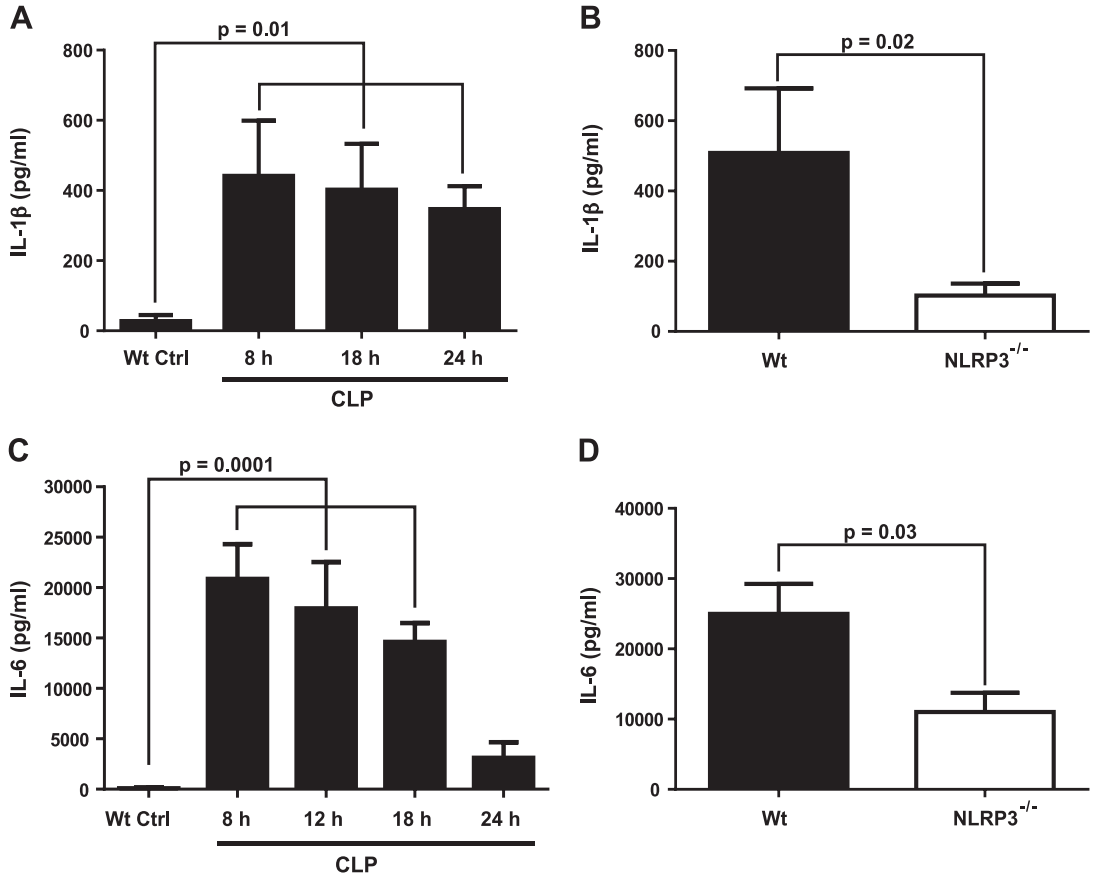

Figure 4. Reduced plasma cytokines in NLRP3$^{-/-}$ mice after CLP. Plasma levels of IL-1β (*A*, *B*) after CLP were reduced in NLRP3 8–24 h after CLP. *A*) Time course of plasma levels of IL-1β after CLP. *B*) Plasma levels of IL-1β were obtained 18 h after CLP. *C*, *D*) A similar protocol was used with a focus on plasma IL-6 8 h after CLP. All assays were performed by ELISA. For each bar, $n \geq 5$ plasma samples.

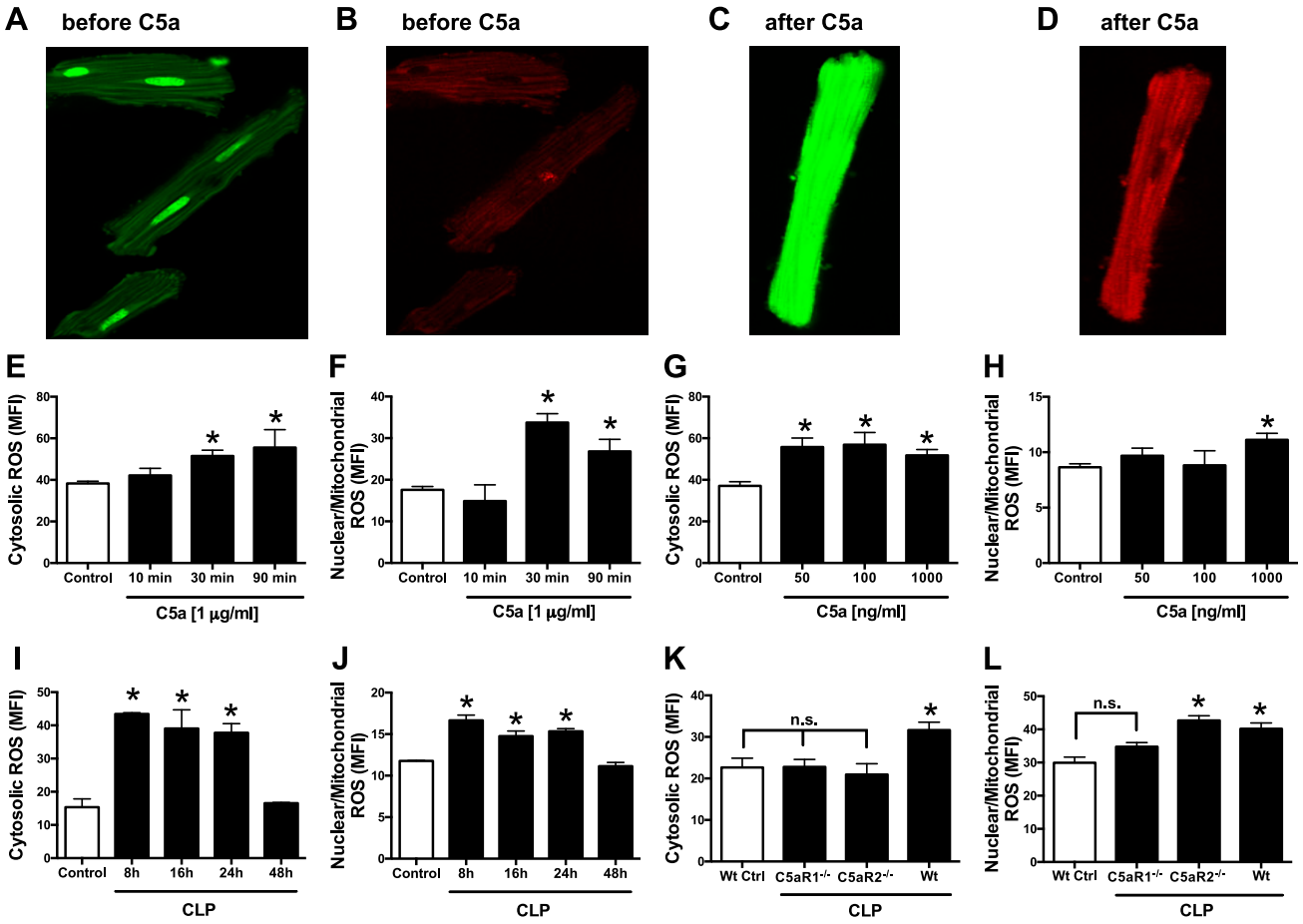

Figure 5. Buildup of ROS in nuclear/mitochondrial and cytosolic areas of CMs. Fluorescent dyes that detect ROS in mitochondria/nuclei (*B*, *D*, *F*, *H*, *J*, *L*) or in cytosol (*A*, *C*, *E*, *G*, *I*, *K*) of rat CMs were used, with endpoints being fluorescence in CMs, as determined by confocal microscopy. *A*, *B*) Sham-procedure CMs exposed to buffer. *C*, *D*) CMs exposed to rC5a (1 μg/ml for 30 min). *E*, *F*) CMs exposed to C5a 10, 30, and 90 min. *G*, *H*) CMs exposed to increasing amounts of C5a for 90 min. *I*, *J*) CMs from WT mice obtained at various time points after CLP. *K*, *L*) CMs obtained from WT, C5aR1$^{-/-}$, and C5aR2$^{-/-}$ mice 16 h after CLP. For each bar, $n > 5$ samples. *$P < 0.05$.

on rat CMs before (Fig. 5*A*, *B*) and after (Fig. 5*C*, *D*) CM exposure to rC5a (1 μg/ml) at 37°C for the indicated periods of time. The fluorescent dyes are cell permeable. The CMs had been preloaded with 2 fluorochromes: the green dye (CellRox Green Reagent), which detects nuclear and mitochondrial ROS, and the red dye (CellRoxDeep Red) which detects cytosolic ROS. (See Material and Methods for details.) Endpoints were obtained by confocal microscopy (Fig. 5*A*–*D*) or by flow cytometry of isolated CMs (Fig. 5*E*–*L*). Before CM exposure to C5a, very low levels of nuclear and mitochondrial ROS staining (green) were found (Fig. 5*A*) and ROS levels of staining (red) in the cytosol (Fig. 5*B*) were barely detectable. In striking contrast, when CMs were exposed *in vitro* to rC5a (1 μg/ml for 30 min) at the indicated time points, there was diffuse green staining for nuclear/mitochondrial ROS (Fig. 5*C*) and moderately intense red staining for cytosolic ROS (Fig. 5*D*). ROS in cytosolic and nuclear/mitochondrial areas was assessed with fluorogenic dyes in CMs exposed *in vitro* to C5a or in CMs at different time points after CLP (Fig. 5*E*–*H*). CMs were exposed to C5a (1 μg/ml) for 10–90 min at 37°C, resulting in a time-dependent progressive increase in cytosolic (Fig. 5*E*) and nuclear/mitochondrial ROS (Fig. 5*F*). Cytosol and nuclear/mitochondrial ROS buildup was assessed as a function of the amount of C5a used for 30 min at 37°C (Fig. 5*G*, *H*). Cytosolic ROS (Fig. 5*G*) was similar at the 3 concentrations of C5a used, whereas nuclear/mitochondrial ROS was found in CMs only at the highest concentration of C5a used (Fig. 5*H*). Buildup of cytosolic and nuclear/mitochondrial ROS in CMs as a function of time after CLP showed an ROS buildup 8–24 h after CLP, followed by decline 48 h after CLP (Fig. 5*I*, *J*). Mice (WT, C5aR1$^{-/-}$, and C5aR2$^{-/-}$) were subjected to polymicrobial sepsis and 18 h later, and their CMs were evaluated by flow cytometry for cytosolic and nuclear/mitochondrial ROS (Fig. 5*K*, *L*). In both locales, there was evidence of C5aR involvement. Buildup of cytosolic ROS required both C5a receptors (Fig. 5*K*), whereas buildup of ROS in a nuclear/mitochondrial location appeared to be more closely linked to C5aR1 (Fig. 5*L*).

Reduced C5a-induced ROS and IL-1β in CMs in the presence of an NOX2 inhibitor

As expected, exposure of rat CMs to C5a (1 μg/ml) caused statistically significant increases in cytosolic (Fig. 6*A*) and

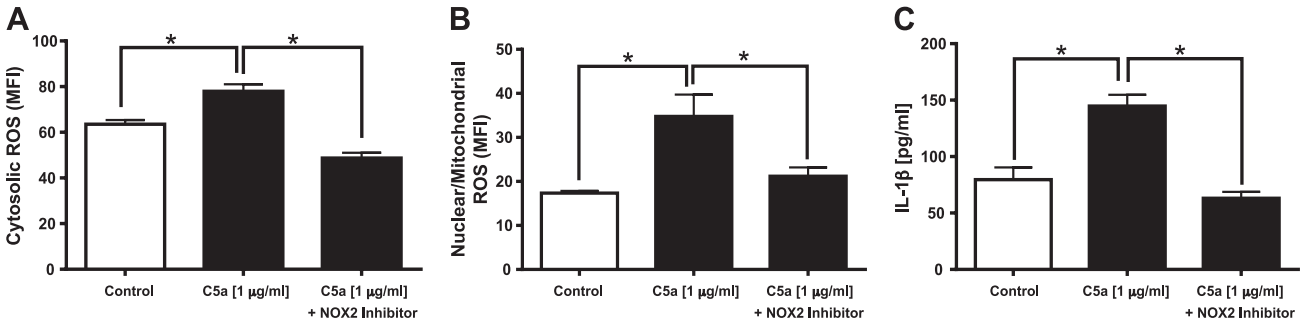

Figure 6. NOX2 inhibitor blocks buildup of ROS in CMs and release of IL-1β. *A*, *B*) Cytosolic ROS (*A*) and nuclear/mitochondrial ROS (*B*) in absence or presence of NOX2 inhibitor in rat CMs exposed to C5a for 1 h at 37°C. *C*) Companion studies focused on IL-1β release from C5a-activated CMs in the presence or absence of NOX2 inhibitor. CMs exposed to C5a for 8 h. For each bar, $n \geq 4$ samples. $^*P < 0.05$.

nuclear/mitochondrial (Fig. 6*B*) ROS, as detected by flow cytometry and by release of IL-1β (Fig. 6*C*). The presence of the NOX2 inhibitor totally suppressed the buildup of cytosolic and nuclear/mitochondrial ROS in CMs. The presence of the NOX2 inhibitor also prevented release of IL-1β from C5a-activated CMs (Fig. 6*C*).

Effects of absence of NLRP3 on sepsis-induced echo/Doppler defects

Selected measures of systolic and diastolic heart function were obtained in mice before and 8 h after CLP (**Fig. 7**). Both WT and NLRP3$^{-/-}$ mice were used. In WT mice, a significant decrease in HR was noted by 8 h after CLP compared to sham-procedure controls (Fig. 7*A*). However, the mild reduction in HR noted in the NLRP3$^{-/-}$ mice at 8 h after CLP was not statistically significant when compared to sham-procedure NLRP3$^{-/-}$ mice. LV SVs were also better preserved in the NLRP3$^{-/-}$ mice after CLP compared to WT (Fig. 7*B*). The higher HR and higher SV resulted in a trend toward a higher (calculated) CO in the NLRP3$^{-/-}$ mice compared to WT at 8 h after CLP (Fig. 7*C*), although the increase did not reach statistical significance. However, the VolS values were also significantly higher in the NLRP3$^{-/-}$ mice than in the WT controls 8 h after CLP, again more closely approximating the LV systolic volume noted in the sham-procedure animals (Fig. 7*D*).

As in our previous studies (3, 26), CLP resulted in a significant reduction in LV volumes (Fig. 7*B*, *D*, *E*), a modest reduction in diastolic function (Fig. 7*F–H*), and a modest increase in systolic function, as measured by LV ejection and shortening fraction 8 h after CLP (data not shown). For each diastolic measure [mitral E/A ratio (Fig. 7*F*), isovolumic relaxation time (Fig. 7*G*), and E/E′sa (Fig. 7*H*)], there was a trend toward better diastolic function in the NLRP3$^{-/-}$ mice compared to controls after CLP, but the differences did not reach statistical significance. In the WT mice, significant differences developed after sepsis, but not in the NLRP3$^{-/-}$ group in the case of isovolumic relaxation time and E/E′sa data. Again, the most substantial cardiovascular effects of CLP were reduction in the

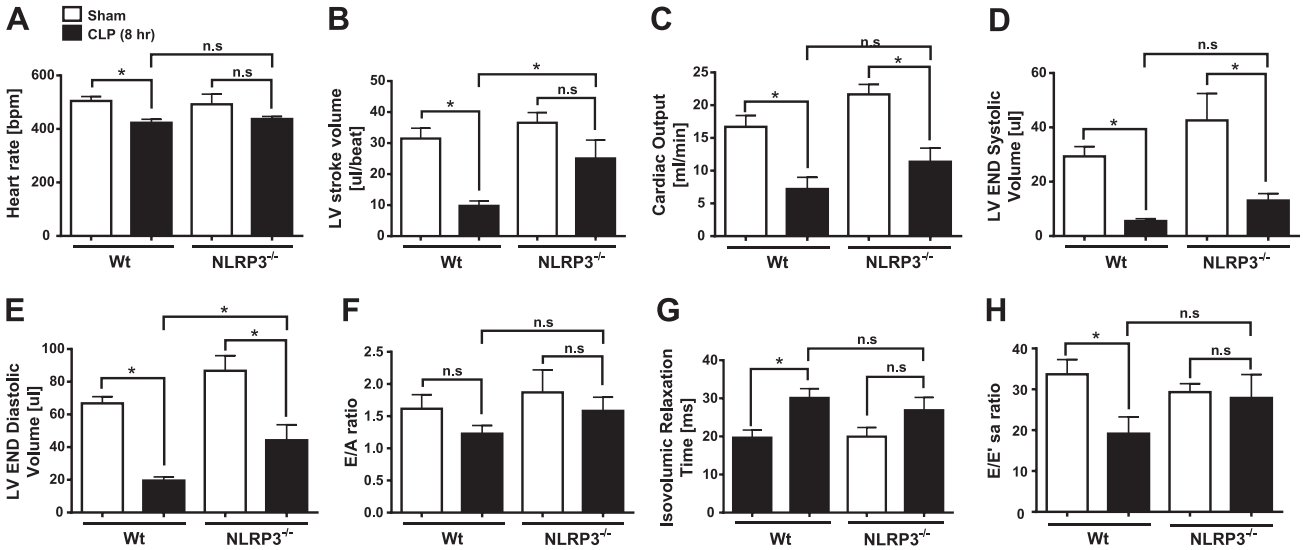

Figure 7. ECHO/Doppler parameters in WT and NLRP3$^{-/-}$ mice 8 h after CLP. HR (*A*), LV SV (*B*), CO (*C*), LV VolS (*D*), LV VolD (*E*), E/A ratio (*F*), isovolumic relaxation (*G*), and E/E′sa (*H*) represent selected measures of systolic and diastolic heart function in mice before and 8 h after CLP. For each bar, $n = 5$ mice. ns, nonsignificant. $^*P < 0.05$.

VolS and VolD, despite fluid resuscitation. At 8 h post-CLP, there was a marked reduction in VolS and VolD, which was less pronounced in the NLRP3$^{-/-}$ mice than in the WT controls (Fig. 7*D*, *E*).

DISCUSSION

NLRP3 inflammasome activation in CMs has been described during viral myocarditis after coxsackievirus B3 infection (35). Inhibition of inflammasome activation with a pan-caspase-1 inhibitor resulted in reduced intensity of myocardial injury in this model along with improved cardiac function. In mice, LPS infusion or *in vitro* presence of LPS with CMs was also associated with myocardial dysfunction (36). In cardiac fibroblasts, the NLRP3 inflammasome was up-regulated in the presence of LPS, in which caspase-1 was activated and IL-1β release occurred (37). In an earlier study, exposure to LPS for 24 h resulted in IL-1β secretion from cardiac fibroblasts, but not from CMs (11).

NLRP3 inflammasome activation in various cell types *in vivo* and *in vitro* has often been associated with TLR2 and -4 binding of DAMPs and PAMPs (38, 39) in which IL-1β was released from monocytes and macrophages after stimulation with a TLR2 or -4 ligand, especially when ATP was used as a secondary stimulus (activator) (9, 40). In macrophages, NLRP3 inflammasome priming with LPS, followed by activation caused by ATP or nigericin necessitated the availability of the purinergic P2X7 receptor and was accompanied with depletion of cytosolic K^+, indicating activation of Na^+/K^+-ATPase (9, 41). ATP has also been found to cause transient pore formation in the cell membrane *via* pannexin-1, allowing DAMPs to cross the plasma membrane and directly activate the NLRP3 inflammasome in the fetus (41). Accordingly, for the current studies, we induced *in vitro* inflammasome model (LPS followed by ATP or nigericin) for inflammasome activation in CMs, resulting in activation of the NLRP3 inflammasome and robust IL-1β release (Fig. 1).

The sublytic membrane attack complex of complement has been found to trigger intracellular Ca^{2+} fluxes, leading to NLRP3 inflammasome activation and loss of the mitochondrial *trans*-membrane potential and activation of caspase-1, resulting in IL-1β release from primary human lung epithelial cells (42) and from murine dendritic cells (19). In human monocytes, C5a in combination with TNF has been shown to prime for cholesterol crystal-induced IL-1β release by increasing IL-1β transcripts and activation of caspase-1 (43) accompanied by C3aR (by C3a) activation which induced IL-1β release by increasing pannexin-1-mediated ATP efflux into the extracellular space (44). C5a was found to prime human retinal pigment epithelial cells for inflammasome activation by lipofuscin-mediated photooxidative damage (20). Further, in earlier studies of rat CMs, IL-1β release was found to be complement dependent (18). In the current report, there was a more than 40-fold increase in NLRP3 and IL-1β mRNA expression during CLP-induced sepsis, which was reduced in the absence of either C5aR1 or -2 (Fig. 3), indicating an activation route for NLRP3 inflammasome in CMs. This result is in line with our immunofluorescent staining data (Fig. 2) indicating that polymicrobial sepsis caused buildup of IL-1β and NLRP3 protein in CMs, which was not present in mice lacking either C5a receptor. Together, these data are consistent with the conclusion that polymicrobial sepsis causes upregulation of the NLRP3 inflammasome (predominately involving NLRP3 and IL-1β mRNAs) in mouse CMs in a manner that requires both C5a receptors. This upregulation may contribute to the harmful events linked to the cardiomyopathy of sepsis. In general, where activation of the NLRP3 inflammasome in the heart has been documented, most studies have associated such events in myocardial fibroblasts and in granulation tissue (containing neutrophils and macrophages) after ischemic–reperfusion injury (45). We documented that, under certain conditions, the NLRP3 inflammasome can be activated in LV CMs and ultimately linked to release of extracellular histones, which have been shown to cause cardiac dysfunction (3). Our recent experiments also showed that plasma extracellular histones were diminished in mice lacking NLRP3 or C5a receptors (3). Such data suggest that the NLRP3 pathway regulates other pathways that lead to NET formation.

Our results suggested that absence of NLRP3 reduced both NLRP3-related cytokines (IL-1β) and non-NLRP3-associated IL-6 (Fig. 4). Because we have previously shown *in vitro* that C5a-activated CMs release TNF, IL-1β, and IL-6 from CLP mice or rats, each of which is known to be cardiosuppressive (18), the reduced level of IL-6 in NLRP3$^{-/-}$ mice may suggest that the NLRP3 inflammasome is involved in CM activation that affects release of IL-1β, as well as IL-6 and TNF. The tertiary structure of NLRP3 containing a highly conserved disulfide bond connecting the pyrin domain is very sensitive to altered redox states (46).

In the current study, we focused on the ability of C5a to activate the NLRP3 inflammasome. The buildup of ROS in CMs after *in vitro* exposure to C5a, as well as after onset of CLP (Fig. 5), indicates a redox imbalance indicative of an oxidative state. Recent studies suggest that CMs exposed to C5a generate ROS from at least 2 different sources (mitochondrial oxidases and cytosolic NOX2) (47). These results suggest that, after CLP, ROS in both cytosolic and nuclear/mitochondrial locales depend on C5a together with the C5a receptors. In CMs, ROS were increased in both locales in the presence of C5a or during sepsis (Fig. 5). Cytosolic ROS buildup in CMs during heart failure has been linked to activation of cytosolic NOX2 (48, 49). Furthermore, NLRP3 was colocalized in mitochondria (42, 50). After inhibition of mitochondrial complex I and III, ROS in mitochondria were increased, together with NLRP3 activation (51, 52). In the present study in CMs, cytosolic and nuclear/mitochondrial ROS generation in response to C5a was attenuated by the NOX2 inhibitor, accompanied by decreased IL-1β release (Fig. 6), suggesting that the NOX2 inhibitor has multiple blocking effects on signaling pathways. (53–55). The results of the present study are in accordance with those in studies showing that inhibition of NADPH oxidase-derived ROS prevents ATP-induced caspase-1 activation and IL-1β release in alveolar macrophages (56). Our findings identify a novel physiologic posttranslational mechanism in the control of NLRP3 inflammasome-mediated inflammatory response in CMs.

The cardiovascular effects of polymicrobial sepsis appear to be significantly reduced in NLRP3$^{-/-}$ mice compared with effects in WT mice, suggesting that the NLRP3 inflammasome mediates some of the effects of sepsis on cardiovascular performance. The effects may be due to a reduction in third-space fluid losses and intravascular volume depletion after CLP. There may also be direct myocardial effects, as noted by a trend toward an improvement in diastolic function (Fig. 7). Together, these data indicate that absence of NLRP3 confers protective effects in cardiovascular compromise after sepsis. Our results are in accordance with earlier studies showing that inhibition of NLRP3 inflammasome by glyburide treatment in mice prevents myocardial dysfunction and reduced levels of plasma IL-1β, together with improved myocardial contractile function in septic mice (37).

In summary, the activated NLRP3 inflammasome is a critical regulator of cardiomyopathy in sepsis. Targeting NLRP3 to attenuate the C5a-induced cardiomyopathy of sepsis may be a feasible therapeutic strategy. FJ

ACKNOWLEDGMENTS

The authors thank Sue Scott and Michelle Possley (University of Michigan) for excellent assistance in the preparation of the manuscript; Peter Radermacher and Enrico Calcia (University of Ulm) for helpful suggestions; Kimber Converso-Baran, research sonographer and echocardiographic specialist (University of Michigan), for excellent services; and the Microscopy and Image-Analysis Laboratory, the Department of Pathology Flow Cytometry Core Facility, and the Department of Cell and Developmental Biology (University of Michigan Medical School) for the use of their facilities. Funding was received from The Endowment for the Basic Sciences. This study was supported by grants from the U.S. National Institutes of Health (NIH), Institute of General Medical Sciences Grants GM-29507 and GM-61656 (to P.A.W.), NIH National Heart, Lung and Blood Institute Grant T32-HL007517 (to J.J.G.), and Deutsche Forschungsgemeinschaft Fellowship Project KA 3740. The authors are responsible for the contents of this publication. The authors declare no conflicts of interest.

AUTHOR CONTRIBUTIONS

M. Kalbitz, F. Fattahi, J. J. Grailer, L. Jajou, E. A. Malan, and F. S. Zetoune performed the experiments; M. Huber-Lang provided advice on experimental protocols; P. A. Ward designed the research protocols and provided overall supervision for all experiments, evaluated the data, and edited the manuscript; M. Kalbitz, F. Fattahi, J. J. Grailer, and F. S. Zetoune wrote and edited the manuscript; M. W. Russell provided interpretation of the ECHO/Doppler data; and all authors collaborated in the interpretation of data and future experimental plans.

REFERENCES

1. Franchi, L., Eigenbrod, T., Muñoz-Planillo, R., and Nuñez, G. (2009) The inflammasome: a caspase-1-activation platform that regulates immune responses and disease pathogenesis. *Nat. Immunol.* **10**, 241–247
2. Stutz, A., Golenbock, D. T., and Latz, E. (2009) Inflammasomes: too big to miss. *J. Clin. Invest.* **119**, 3502–3511
3. Kalbitz, M., Grailer, J. J., Fattahi, F., Jajou, L., Herron, T. J., Campbell, K. F., Zetoune, F. S., Bosmann, M., Sarma, J. V., Huber-Lang, M., Gebhard, F., Loaiza, R., Valdivia, H. H., Jalife, J., Russell, M. W., and Ward, P. A. (2015) Role of extracellular histones in the cardiomyopathy of sepsis. *FASEB J.* **29**, 2185–2193
4. Martinon, F., Pétrilli, V., Mayor, A., Tardivel, A., and Tschopp, J. (2006) Gout-associated uric acid crystals activate the NALP3 inflammasome. *Nature* **440**, 237–241
5. Duewell, P., Kono, H., Rayner, K. J., Sirois, C. M., Vladimer, G., Bauernfeind, F. G., Abela, G. S., Franchi, L., Nuñez, G., Schnurr, M., Espevik, T., Lien, E., Fitzgerald, K. A., Rock, K. L., Moore, K. J., Wright, S. D., Hornung, V., and Latz, E. (2010) NLRP3 inflammasomes are required for atherogenesis and activated by cholesterol crystals. *Nature* **464**, 1357–1361
6. Xiang, M., Shi, X., Li, Y., Xu, J., Yin, L., Xiao, G., Scott, M. J., Billiar, T. R., Wilson, M. A., and Fan, J. (2011) Hemorrhagic shock activation of NLRP3 inflammasome in lung endothelial cells. *J. Immunol.* **187**, 4809–4817
7. Muñoz-Planillo, R., Franchi, L., Miller, L. S., and Núñez, G. (2009) A critical role for hemolysins and bacterial lipoproteins in Staphylococcus aureus-induced activation of the Nlrp3 inflammasome. *J. Immunol.* **183**, 3942–3948
8. Kim, S., Bauernfeind, F., Ablasser, A., Hartmann, G., Fitzgerald, K. A., Latz, E., and Hornung, V. (2010) Listeria monocytogenes is sensed by the NLRP3 and AIM2 inflammasome. *Eur. J. Immunol.* **40**, 1545–1551
9. Mariathasan, S., Weiss, D. S., Newton, K., McBride, J., O'Rourke, K., Roose-Girma, M., Lee, W. P., Weinrauch, Y., Monack, D. M., and Dixit, V. M. (2006) Cryopyrin activates the inflammasome in response to toxins and ATP. *Nature* **440**, 228–232
10. Mezzaroma, E., Toldo, S., Farkas, D., Seropian, I. M., Van Tassell, B. W., Salloum, F. N., Kannan, H. R., Menna, A. C., Voelkel, N. F., and Abbate, A. (2011) The inflammasome promotes adverse cardiac remodeling following acute myocardial infarction in the mouse. *Proc. Natl. Acad. Sci. USA* **108**, 19725–19730
11. Kawaguchi, M., Takahashi, M., Hata, T., Kashima, Y., Usui, F., Morimoto, H., Izawa, A., Takahashi, Y., Masumoto, J., Koyama, J., Hongo, M., Noda, T., Nakayama, J., Sagara, J., Taniguchi, S., and Ikeda, U. (2011) Inflammasome activation of cardiac fibroblasts is essential for myocardial ischemia/reperfusion injury. *Circulation* **123**, 594–604
12. Pomerantz, B. J., Reznikov, L. L., Harken, A. H., and Dinarello, C. A. (2001) Inhibition of caspase 1 reduces human myocardial ischemic dysfunction via inhibition of IL-18 and IL-1beta. *Proc. Natl. Acad. Sci. USA* **98**, 2871–2876
13. Bracey, N. A., Beck, P. L., Muruve, D. A., Hirota, S. A., Guo, J., Jabagi, H., Wright, J. R., Jr., Macdonald, J. A., Lees-Miller, J. P., Roach, D., Semeniuk, L. M., and Duff, H. J. (2013) The Nlrp3 inflammasome promotes myocardial dysfunction in structural cardiomyopathy through interleukin-1β. *Exp. Physiol.* **98**, 462–472
14. Hwang, M. W., Matsumori, A., Furukawa, Y., Ono, K., Okada, M., Iwasaki, A., Hara, M., Miyamoto, T., Touma, M., and Sasayama, S. (2001) Neutralization of interleukin-1beta in the acute phase of myocardial infarction promotes the progression of left ventricular remodeling. *J. Am. Coll. Cardiol.* **38**, 1546–1553
15. Suzuki, K., Murtuza, B., Smolenski, R. T., Sammut, I. A., Suzuki, N., Kaneda, Y., and Yacoub, M. H. (2001) Overexpression of interleukin-1 receptor antagonist provides cardioprotection against ischemia-reperfusion injury associated with reduction in apoptosis. *Circulation* **104**(Suppl. 1), I308–I313
16. Abbate, A., Van Tassell, B. W., Seropian, I. M., Toldo, S., Robati, R., Varma, A., Salloum, F. N., Smithson, L., and Dinarello, C. A. (2010) Interleukin-1beta modulation using a genetically engineered antibody prevents adverse cardiac remodelling following acute myocardial infarction in the mouse. *Eur. J. Heart Fail.* **12**, 319–322
17. Maass, D. L., White, J., and Horton, J. W. (2002) IL-1beta and IL-6 act synergistically with TNF-alpha to alter cardiac contractile function after burn trauma. *Shock* **18**, 360–366
18. Atefi, G., Zetoune, F. S., Herron, T. J., Jalife, J., Bosmann, M., Al-Aref, R., Sarma, J. V., and Ward, P. A. (2011) Complement dependency of cardiomyocyte release of mediators during sepsis. *FASEB J.* **25**, 2500–2508
19. Laudisi, F., Spreafico, R., Evrard, M., Hughes, T. R., Mandriani, B., Kandasamy, M., Morgan, B. P., Sivasankar, B., and Mortellaro, A. (2013) Cutting edge: the NLRP3 inflammasome links complement-mediated inflammation and IL-1β release. *J. Immunol.* **191**, 1006–1010
20. Brandstetter, C., Holz, F. G., and Krohne, T. U. (2015) Complement component C5a primes retinal pigment epithelial cells for

inflammasome activation by lipofuscin-mediated photooxidative damage. *J. Biol. Chem.* **290**, 31189–31198
21. Ward, P. A., Guo, R. F., and Riedemann, N. C. (2012) Manipulation of the complement system for benefit in sepsis. *Crit. Care Res. Pract.* **2012**, 427607
22. Goldhaber, J. I., Kim, K. H., Natterson, P. D., Lawrence, T., Yang, P., and Weiss, J. N. (1996) Effects of TNF-alpha on [Ca2+]i and contractility in isolated adult rabbit ventricular myocytes. *Am. J. Physiol.* **271**, H1449–H1455
23. Niederbichler, A. D., Hoesel, L. M., Westfall, M. V., Gao, H., Ipaktchi, K. R., Sun, L., Zetoune, F. S., Su, G. L., Arbabi, S., Sarma, J. V., Wang, S. C., Hemmila, M. R., and Ward, P. A. (2006) An essential role for complement C5a in the pathogenesis of septic cardiac dysfunction. *J. Exp. Med.* **203**, 53–61
24. Rittirsch, D., Flierl, M. A., Nadeau, B. A., Day, D. E., Huber-Lang, M., Mackay, C. R., Zetoune, F. S., Gerard, N. P., Cianflone, K., Köhl, J., Gerard, C., Sarma, J. V., and Ward, P. A. (2008) Functional roles for C5a receptors in sepsis. *Nat. Med.* **14**, 551–557
25. Hoesel, L. M., Niederbichler, A. D., Schaefer, J., Ipaktchi, K. R., Gao, H., Rittirsch, D., Pianko, M. J., Vogt, P. M., Sarma, J. V., Su, G. L., Arbabi, S., Westfall, M. V., Wang, S. C., Hemmila, M. R., and Ward, P. A. (2007) C5a-blockade improves burn-induced cardiac dysfunction. *J. Immunol.* **178**, 7902–7910
26. Kalbitz, M., Fattahi, F., Grailer, J. J., Jajou, L., Malan, E. A., Zetoune, F. S., Huber-Lang, M., Russell, M. W., and Ward, P. A. (2016) Complement destabilizes cardiomyocyte function in vivo after polymicrobial sepsis and in vitro. [E-pub ahead of print] *J. Immunol.* doi:10.4049/jimmunol.1600091
27. Kaestner, L., Scholz, A., Hammer, K., Vecerdea, A., Ruppenthal, S., and Lipp, P. (2009) Isolation and genetic manipulation of adult cardiac myocytes for confocal imaging. *J. Vis. Exp.* 31, 1433
28. Louch, W. E., Sheehan, K. A., and Wolska, B. M. (2011) Methods in cardiomyocyte isolation, culture, and gene transfer. *J. Mol. Cell. Cardiol.* **51**, 288–298
29. Höpken, U. E., Lu, B., Gerard, N. P., and Gerard, C. (1996) The C5a chemoattractant receptor mediates mucosal defence to infection. *Nature* **383**, 86–89
30. Gerard, N. P., Lu, B., Liu, P., Craig, S., Fujiwara, Y., Okinaga, S., and Gerard, C. (2005) An anti-inflammatory function for the complement anaphylatoxin C5a-binding protein, C5L2. *J. Biol. Chem.* **280**, 39677–39680
31. Baker, C. C., Chaudry, I. H., Gaines, H. O., and Baue, A. E. (1983) Evaluation of factors affecting mortality rate after sepsis in a murine cecal ligation and puncture model. *Surgery* **94**, 331–335
32. Rittirsch, D., Huber-Lang, M. S., Flierl, M. A., and Ward, P. A. (2009) Immunodesign of experimental sepsis by cecal ligation and puncture. *Nat. Protoc.* **4**, 31–36
33. Huber-Lang, M., Sarma, V. J., Lu, K. T., McGuire, S. R., Padgaonkar, V. A., Guo, R. F., Younkin, E. M., Kunkel, R. G., Ding, J., Erickson, R., Curnutte, J. T., and Ward, P. A. (2001) Role of C5a in multiorgan failure during sepsis. *J. Immunol.* **166**, 1193–1199
34. Boluyt, M. O., Converso, K., Hwang, H. S., Mikkor, A., and Russell, M. W. (2004) Echocardiographic assessment of age-associated changes in systolic and diastolic function of the female F344 rat heart. *J. Appl. Physiol.* **96**, 822–828
35. Wang, Y., Gao, B., and Xiong, S. (2014) Involvement of NLRP3 inflammasome in CVB3-induced viral myocarditis. *Am. J. Physiol. Heart Circ. Physiol.* **307**, H1438–H1447
36. Boyd, J. H., Mathur, S., Wang, Y., Bateman, R. M., and Walley, K. R. (2006) Toll-like receptor stimulation in cardiomyoctes decreases contractility and initiates an NF-kappaB dependent inflammatory response. *Cardiovasc. Res.* **72**, 384–393
37. Zhang, W., Xu, X., Kao, R., Mele, T., Kvietys, P., Martin, C. M., and Rui, T. (2014) Cardiac fibroblasts contribute to myocardial dysfunction in mice with sepsis: the role of NLRP3 inflammasome activation. *PLoS One* **9**, e107639
38. Lacroix-Lamandé, S., d'Andon, M. F., Michel, E., Ratet, G., Philpott, D. J., Girardin, S. E., Boneca, I. G., Vandewalle, A., and Werts, C. (2012) Downregulation of the Na/K-ATPase pump by leptospiral glycolipoprotein activates the NLRP3 inflammasome. *J. Immunol.* **188**, 2805–2814
39. Witzenrath, M., Pache, F., Lorenz, D., Koppe, U., Gutbier, B., Tabeling, C., Reppe, K., Meixenberger, K., Dorhoi, A., Ma, J., Holmes, A., Trendelenburg, G., Heimesaat, M. M., Bereswill, S., van der Linden, M., Tschopp, J., Mitchell, T. J., Suttorp, N., and Opitz, B. (2011) The NLRP3 inflammasome is differentially activated by pneumolysin variants and contributes to host defense in pneumococcal pneumonia. *J. Immunol.* **187**, 434–440
40. Netea, M. G., Nold-Petry, C. A., Nold, M. F., Joosten, L. A., Opitz, B., van der Meer, J. H., van de Veerdonk, F. L., Ferwerda, G., Heinhuis, B., Devesa, I., Funk, C. J., Mason, R. J., Kullberg, B. J., Rubartelli, A., van der Meer, J. W., and Dinarello, C. A. (2009) Differential requirement for the activation of the inflammasome for processing and release of IL-1beta in monocytes and macrophages. *Blood* **113**, 2324–2335
41. Pelegrin, P., and Surprenant, A. (2006) Pannexin-1 mediates large pore formation and interleukin-1beta release by the ATP-gated P2X7 receptor. *EMBO J.* **25**, 5071–5082
42. Triantafilou, K., Hughes, T. R., Triantafilou, M., and Morgan, B. P. (2013) The complement membrane attack complex triggers intracellular Ca2+ fluxes leading to NLRP3 inflammasome activation. *J. Cell Sci.* **126**, 2903–2913
43. Samstad, E. O., Niyonzima, N., Nymo, S., Aune, M. H., Ryan, L., Bakke, S. S., Lappegård, K. T., Brekke, O. L., Lambris, J. D., Damås, J. K., Latz, E., Mollnes, T. E., and Espevik, T. (2014) Cholesterol crystals induce complement-dependent inflammasome activation and cytokine release. *J. Immunol.* **192**, 2837–2845
44. Asgari, E., Le Friec, G., Yamamoto, H., Perucha, E., Sacks, S. S., Köhl, J., Cook, H. T., and Kemper, C. (2013) C3a modulates IL-1β secretion in human monocytes by regulating ATP efflux and subsequent NLRP3 inflammasome activation. *Blood* **122**, 3473–3481
45. Sandanger, Ø., Ranheim, T., Vinge, L. E., Bliksøen, M., Alfsnes, K., Finsen, A. V., Dahl, C. P., Askevold, E. T., Florholmen, G., Christensen, G., Fitzgerald, K. A., Lien, E., Valen, G., Espevik, T., Aukrust, P., and Yndestad, A. (2013) The NLRP3 inflammasome is up-regulated in cardiac fibroblasts and mediates myocardial ischaemia-reperfusion injury. *Cardiovasc. Res.* **99**, 164–174
46. Bae, J. Y., and Park, H. H. (2011) Crystal structure of NALP3 protein pyrin domain (PYD) and its implications in inflammasome assembly. *J. Biol. Chem.* **286**, 39528–39536
47. Dikalov, S. (2011) Cross talk between mitochondria and NADPH oxidases. *Free Radic. Biol. Med.* **51**, 1289–1301
48. Cave, A., Grieve, D., Johar, S., Zhang, M., and Shah, A. M. (2005) NADPH oxidase-derived reactive oxygen species in cardiac pathophysiology. *Philos. Trans. R. Soc. Lond. B Biol. Sci.* **360**, 2327–2334
49. Hingtgen, S. D., Tian, X., Yang, J., Dunlay, S. M., Peek, A. S., Wu, Y., Sharma, R. V., Engelhardt, J. F., and Davisson, R. L. (2006) Nox2-containing NADPH oxidase and Akt activation play a key role in angiotensin II-induced cardiomyocyte hypertrophy. *Physiol. Genomics* **26**, 180–191
50. Bracey, N. A., Gershkovich, B., Chun, J., Vilaysane, A., Meijndert, H. C., Wright, J. R., Jr., Fedak, P. W., Beck, P. L., Muruve, D. A., and Duff, H. J. (2014) Mitochondrial NLRP3 protein induces reactive oxygen species to promote Smad protein signaling and fibrosis independent from the inflammasome. *J. Biol. Chem.* **289**, 19571–19584
51. Bulua, A. C., Simon, A., Maddipati, R., Pelletier, M., Park, H., Kim, K. Y., Sack, M. N., Kastner, D. L., and Siegel, R. M. (2011) Mitochondrial reactive oxygen species promote production of proinflammatory cytokines and are elevated in TNFR1-associated periodic syndrome (TRAPS). *J. Exp. Med.* **208**, 519–533
52. Zhou, R., Yazdi, A. S., Menu, P., and Tschopp, J. (2011) A role for mitochondria in NLRP3 inflammasome activation. *Nature* **469**, 221–225
53. Sadek, H. A., Szweda, P. A., and Szweda, L. I. (2004) Modulation of mitochondrial complex I activity by reversible Ca2+ and NADH mediated superoxide anion dependent inhibition. *Biochemistry* **43**, 8494–8502
54. Fato, R., Bergamini, C., Bortolus, M., Maniero, A. L., Leoni, S., Ohnishi, T., and Lenaz, G. (2009) Differential effects of mitochondrial Complex I inhibitors on production of reactive oxygen species. *Biochim. Biophys. Acta* **1787**, 384–392
55. Khan, S. A., Nanduri, J., Yuan, G., Kinsman, B., Kumar, G. K., Joseph, J., Kalyanaraman, B., and Prabhakar, N. R. (2011) NADPH oxidase 2 mediates intermittent hypoxia-induced mitochondrial complex I inhibition: relevance to blood pressure changes in rats. *Antioxid. Redox Signal.* **14**, 533–542
56. Cruz, C. M., Rinna, A., Forman, H. J., Ventura, A. L., Persechini, P. M., and Ojcius, D. M. (2007) ATP activates a reactive oxygen species-dependent oxidative stress response and secretion of proinflammatory cytokines in macrophages. *J. Biol. Chem.* **282**, 2871–2879

Received for publication June 9, 2016.
Accepted for publication August 8, 2016.